

A Lucky Imaging search for stellar sources near 74 transit hosts[★]

Maria Wöllert¹ and Wolfgang Brandner¹

Max-Planck-Institut für Astronomie, Königstuhl 17, 69117 Heidelberg, Germany
e-mail: woellert@mpia.de

Received —; accepted —

ABSTRACT

Context. Many transiting planet host stars lack high resolution imaging and thus close stellar sources can be missed. Those unknown stars potentially bias the derivation of the planetary and stellar parameters from the transit light curve, no matter if they are bound or not. In addition, bound stellar companions interact gravitationally with the exoplanet host star, the disk and the planets and can thus influence the formation and evolution of the planetary system strongly.

Aims. We extended our high-resolution Lucky Imaging survey for close stellar sources by 74 transiting planet host stars. 39 of these stars lack previous high-resolution imaging, 23 are follow up observations of companions or companion candidates, and the remaining stars have been observed by others with AO imaging though in different bands. We determine the separation of all new and known companion candidates and estimate the flux ratio in the observed bands.

Methods. All observations were carried out with the Lucky Imaging camera AstraLux Norte at the Calar Alto 2.2 m telescope in i' and z' passbands.

Results. We find new stellar sources within $1''$ to HAT-P-27, HAT-P-28, HAT-P-35, WASP-76, and WASP-103 and between $1''$ and $4''$ to HAT-P-29, and WASP-56.

Key words. Techniques: high angular resolution – Binaries: visual – Planetary systems

1. Introduction

During the last 15 years, more than 1000 confirmed and several 1000 candidate exoplanets have been found by ground- and space-based transit searches as HATNet (Bakos et al. 2004), SuperWasp (Pollacco et al. 2006), CoRoT (Baglin et al. 2006), and Kepler (Borucki et al. 2010; Batalha et al. 2013; Burke et al. 2014). Transiting exoplanets (TEPs) offer the unique opportunity to determine a variety of planetary properties as true mass, mean density and surface gravity. They also allow to characterize the planet's atmosphere through spectroscopy, to determine the planet's temperature in secondary eclipse observations, and to measure the angle between the orbital plane and the stellar rotation axis via the Rossiter-McLaughlin effect (Winn et al. 2005).

As many transiting planet follow-up observations were limited in angular resolution either due to instrumental limits (like, e.g., SPITZER/IRAC) or - in case of ground-based follow-up - seeing limited, care has to be taken about missing a blended close star. This is especially true for faint sources as bright stars may be recognized in follow-up spectra. Unknown, close stars add a constant flux to the light-curve which bias both, primary and secondary eclipse measurements. In the first case, the additional source leads to an underestimate of the planetary radius and consequently an overestimate of the planetary density. In the second case, the planet infrared emission spectrum can be underestimated by several tens of percent (e.g. Crossfield et al. 2012).

Finding close stellar sources to transiting exoplanet host stars is, however, not only crucial to determine the planetary parameters correctly, but also to understand the influence of binarity on

the formation and evolution of planetary systems. Even though not all of the detected, close stars are gravitationally bound, a lot of them are as has been shown via multi-epoch high-resolution observations (e.g. Narita et al. 2012; Bergfors et al. 2013; Ngo et al. 2015). The effects of binarity may be manifold: Stellar companions might stir (Mayer et al. 2005), tilt (Batygin 2012) or truncate the protoplanetary disk (Artymowicz & Lubow 1994) or they can interact with the formed planets via, e.g., the Lidov-Kozai mechanism or other secular interactions (Wu & Murray 2003; Fabrycky & Tremaine 2007; Naoz et al. 2011). Stellar companions may be thus one important cause for the observed variety of planetary system architectures.

Several groups have already done systematic surveys for stellar companions using either the Lucky Imaging method (e.g. Daemgen et al. 2009; Faedi et al. 2013; Bergfors et al. 2013; Lillo-Box et al. 2012, 2014; Wöllert et al. 2015), speckle imaging (e.g. Howell et al. 2011; Horch et al. 2014; Kane et al. 2014; Everett et al. 2015), AO-assisted imaging on its own, or combined with radial velocity methods (e.g. Adams et al. 2012, 2013; Guenther et al. 2013; Dressing et al. 2014; Law et al. 2014; Wang et al. 2014; Ngo et al. 2015), or search for colour-dependency of the transit depths (e.g. Colón et al. 2012; Désert et al. 2015). However, more and more transiting exoplanets are found and their precise characterisation will enable us to get a more precise view at the important mechanisms that shape planetary systems.

In this paper we present the results of our ongoing effort to find stellar sources close to TEP host stars. The observations and data reductions were performed similarly to our previous paper Wöllert et al. (2015) and are briefly described in Section 2. In Section 3 we present the astrometric and photometric properties of the observed sources and we summarize our findings in Section 4.

[★] Based on observations collected at the German-Spanish Astronomical Center, Calar Alto, jointly operated by the Max-Planck-Institut für Astronomie Heidelberg and the Instituto de Astrofísica de Andalucía (CSIC).

2. Observations and data reduction

2.1. Sample selection

The initial motivation for our survey was to focus on TEPs with already existing measurements of the Rossiter-McLaughlin effect, and to explore a possible relationship of the angle defined by the spin vectors of the TEP host star and the planetary orbit, and the presence or absence of a stellar companion. This selection criterion was later relaxed to include all TEP host stars sufficiently bright ($i \leq 13$ mag) to facilitate high-quality Lucky Imaging. The majority of the targets were selected from TEPs either identified by the SuperWASP or the HatNet project. This was complemented by TEP hosts identified in other ground- or space-based surveys. We focused on stars without previous high-angular resolution observations, as well as on TEP host stars with previous detections of stellar companion candidates in order to derive constraints on the relative astrometry between TEP host and stellar companion candidate.

2.2. Lucky Imaging with AstraLux at Calar Alto

All observations were carried out at Calar Alto with the 2.2 m telescope in combination with the Lucky Imaging camera AstraLux Norte (Hormuth et al. 2008) during two observing runs, one night in October 2014 and three nights in March 2015. The targets were observed in SDSS i' and z' -passbands using the same set-up as described in Wöllert et al. (2015). The field of view was $12''$ by $12''$ with the exoplanet host star separated at least $4''$ from the image borders. Depending on the target brightness and observing conditions we took between 10000 and 54000 individual frames with exposure times of 15 ms each so that the probability of getting a stable speckle pattern is sufficiently large. The individual AstraLux images are dark subtracted and flat-fielded. For the data analysis we chose the 10% of images with the highest Strehl ratio and combined them using the shift-and-add technique.

In order to precisely measure the separation and position angle of the companion candidates we took at least 3 images of the globular cluster M13 each night. Using IRAF imexamine we determined the detector position of 5 widely separated stars in the field and calculated their separation and rotation angle pairwise. The result was compared to the values from high-quality astrometric HST/ACS observations. As the instrument was not unmounted during the observing nights in March 2015, we used the images of all three nights for the calibration of that run. The plate scale and detector rotation were 23.46 ± 0.01 mas/px and $1.7^\circ \pm 0.1^\circ$ west of north and 23.51 ± 0.01 mas/px and $2.0^\circ \pm 0.1^\circ$ west of north for the observations in October 2014 and March 2015, respectively.

2.3. Photometry and astrometry

To find all stellar sources, also those which are faint and close to the transiting planet host star, we first subtracted the point spread function (PSF) of the TEP host. As the PSFs vary significantly from image to image and no standard PSF can be used for all observations, we fitted a theoretical model PSF to each star. The theoretical model PSF comprises the PSF from an ideal telescope without atmosphere which is then convolved with a Gaussian and finally added to a Moffat profile. The model also weights the two PSF components (see Wöllert et al. 2014, for more information on the procedure). If a companion candidate was found, we fitted a scaled and differently weighted PSF to

it to determine its position and the flux ratio of the two components. We used the PSF subtracted images additionally to calculate the 5σ -contrast curve. For this purpose, we divided the flux in a box of 5×5 pixel around each pixel by the flux of star in a similarly sized box centred on the peak in the original, not PSF subtracted image. The contrast at a specific separation is then calculated as the median of the contrast of all pixels at the corresponding separation. The contrast at $r = 0.25'', 0.5'', 1.0'',$ and $2.0''$ of targets with candidate companions is given in Table 1, the contrast for all other targets is given in Table 2. Outside of $2.0''$, the contrast decreases only very little and the value given for $2.0''$ can be assumed.

The flux ratio in both passbands was measured using the IDL routine APER which performs aperture photometry. We used an aperture size of 4.5 px which is about the full width half maximum of the stellar PSFs. In contrast to the usual approach, the sky background was not measured in a close annulus around the star, but in a 50×50 px sized box in one corner of the image without stellar source for the primary and at the opposite position of the TEP host with the same distance and aperture size for the fainter companion. This ensures that the flux contribution of the brighter TEP host is accurately subtracted from those of the fainter source as our PSFs are almost point symmetrical in shape. The uncertainties of the flux ratios are propagated from the statistical photometric errors given by APER and systematic errors from using this method. The latter were estimated by comparing the results obtained by using different aperture sizes as well as the flux ratios determined by PSF-fitting.

3. Results

To the 74 observed TEP host stars we find new companion candidates to HAT-P-27, HAT-P-28, HAT-P-35, WASP-76, and WASP-103 within $1''$, to HAT-P-29 and WASP-56 within $4''$, and the candidates of HAT-P-15, HAT-P-54, and Kepler-89 are situated outside of $4''$. Images in z' of all these sources can be found in Figure 1. In addition, we did follow-up observations of 23 already known companion candidates. The astrometric positions and flux ratios in i' and z' of all companion candidates can be found in Table 3.

As can be seen in Table 3, most sources appear to be redder than the primary which would be expected for a lower mass companion. The uncertainties are, however, too large to allow a precise estimate of the spectral type. To achieve this, adaptive optics based observations or spectra would be needed. The knowledge of the companion candidate spectral type would then allow to correct the planetary parameter and infrared emission spectra of the new close companions, as well as to compare their photometric distance to those of the TEP host star to investigate whether the sources may be gravitationally bound or not. For this purpose their astrometric position needs to be followed up in the upcoming years as well.

4. Summary

In our ongoing Lucky Imaging search for stellar sources close to transiting exoplanet host stars we identified 5 new, close sources within $1''$ to HAT-P-27, HAT-P-28, HAT-P-35, WASP-76, and WASP-103 which have been overlooked so far. The planetary and stellar parameters and thermal radiation profile of the transiting planets of these sources may have to be corrected according to the spectral type of the companion candidate star which remains to be determined. Also the detected companion candidates to HAT-P-29 and WASP-56 which are located at $3.3''$ and

Table 1: TEP hosts with detection, radial contrast limits, references to other high-resolution imaging papers if available

Name	5σ detection limit ($\Delta z'$ [mag])				ref.
	0.25''	0.5''	1.0''	2.0''	
New companion candidates					
HAT-P-15	4.28	5.37	6.40	6.90	Ngo et al. (2015)*
HAT-P-27/WASP-40	3.90	4.82	5.75	6.20	Wöllert et al. (2015)*
HAT-P-28	3.24	3.94	4.76	5.12	
HAT-P-29	4.05	4.72	5.45	5.95	Ngo et al. (2015)*
HAT-P-35	2.81	3.37	3.94	4.11	
HAT-P-54	3.57	4.41	5.13	5.52	
Kepler-89	3.10	3.60	4.28	4.69	Adams et al. (2012)*; Lillo-Box et al. (2014)*
WASP-56	4.08	4.89	5.78	6.11	
WASP-76	3.81	4.79	6.21	7.18	
WASP-103	3.75	4.55	5.48	5.90	
Known companion candidates					
CoRoT-02	2.97	3.46	4.16	4.78	Alonso et al. (2008); Faedi et al. (2013); Wöllert et al. (2015)
CoRoT-03	2.85	3.22	3.65	3.97	Deleuil et al. (2008); Faedi et al. (2013); Wöllert et al. (2015)
CoRoT-11	3.25	3.85	4.65	4.97	Gandolfi et al. (2010); Wöllert et al. (2015)
HAT-P-20	3.64	4.30	5.22	5.97	Ngo et al. (2015)*; Bakos et al. (2011) [†]
HAT-P-24	3.51	4.39	5.11	5.67	Ngo et al. (2015)
HAT-P-30	4.01	5.06	6.09	6.72	Adams et al. (2013); Ngo et al. (2015)
HAT-P-32	3.78	4.61	5.35	5.84	Adams et al. (2013); Ngo et al. (2015); Wöllert et al. (2015)*
HAT-P-41	3.24	3.62	4.37	4.97	Hartman et al. (2012); Wöllert et al. (2015)
KELT-2	3.75	4.61	6.13	7.03	Beatty et al. (2012) [†]
KELT-3	3.95	4.75	5.45	5.95	Pepper et al. (2013)
Kepler-13	3.33	4.11	4.87	5.54	Santerne et al. (2012)
KIC10905746	3.33	3.78	4.56	5.09	Fischer et al. (2012)
LHS-6343	2.72	3.19	3.73	4.40	Johnson et al. (2011); Montet et al. (2015)
TrES-4	6.13	6.09	6.07	6.13	Daemgen et al. (2009); Bergfors et al. (2013); Faedi et al. (2013); Wöllert et al. (2015); Ngo et al. (2015)
WASP-11	3.80	4.81	5.70	6.25	Ngo et al. (2015)
WASP-12	4.03	4.78	5.56	6.12	Crossfield et al. (2012); Bergfors et al. (2013); Bechter et al. (2014)
WASP-14	4.26	5.29	6.82	7.70	Wöllert et al. (2015); Ngo et al. (2015)
WASP-33	3.33	4.77	6.64	7.90	Moya et al. (2011); Adams et al. (2013)
WASP-36	3.38	4.34	4.84	5.16	Smith et al. (2012) [†]
WASP-70	3.07	3.52	4.26	4.90	Anderson et al. (2014) [†]
WASP-77	3.71	4.54	5.60	6.42	Maxted et al. (2013)
WASP-85	4.25	5.26	6.21	7.12	Brown et al. (2014) [†]
XO-3	4.11	4.91	5.79	6.33	Bergfors et al. (2013); Adams et al. (2013); Ngo et al. (2015)*

*: Outside FoV, *: no detection, †: seeing limited observation or catalog data

3.4'' respectively to the TEP host could have this influence as the photometric aperture used for the transit observations, e.g. with SPITZER, are about that size. The sources that are outside of 4'' to HAT-P-15, HAT-P-54, and Kepler-89 do not influence the planetary and stellar property derivation from transit light curve, but can be of interest if they happen to be bound to the TEP host. This needs to be investigated with astrometric observations over the upcoming years. In this work, we also give the astrometric positions and i' and z' flux ratios of 23 already known companion candidates.

Acknowledgements. MW acknowledges support by the International Max Planck Research School for Astronomy & Cosmic Physics in Heidelberg (IMPRS-HD).

References

Adams, E. R., Ciardi, D. R., Dupree, A. K., et al. 2012, *AJ*, 144, 42
 Adams, E. R., Dupree, A. K., Kulesa, C., & McCarthy, D. 2013, *AJ*, 146, 9
 Alonso, R., Auvergne, M., Baglin, A., et al. 2008, *A&A*, 482, L21
 Anderson, D. R., Collier Cameron, A., Delrez, L., et al. 2014, *MNRAS*, 445, 1114
 Artymowicz, P. & Lubow, S. H. 1994, *ApJ*, 421, 651

Baglin, A., Auvergne, M., Barge, P., et al. 2006, in *ESA Special Publication*, Vol. 1306, *ESA Special Publication*, ed. M. Fridlund, A. Baglin, J. Lochard, & L. Conroy, 33
 Bakos, G., Noyes, R. W., Kovács, G., et al. 2004, *PASP*, 116, 266
 Bakos, G. Á., Hartman, J., Torres, G., et al. 2011, *ApJ*, 742, 116
 Batalha, N. M., Rowe, J. F., Bryson, S. T., et al. 2013, *ApJS*, 204, 24
 Batygin, K. 2012, *Nature*, 491, 418
 Beatty, T. G., Pepper, J., Siverd, R. J., et al. 2012, *ApJ*, 756, L39
 Bechter, E. B., Crepp, J. R., Ngo, H., et al. 2014, *ApJ*, 788, 2
 Bergfors, C., Brandner, W., Daemgen, S., et al. 2013, *MNRAS*, 428, 182
 Bieryla, A., Collins, K., Beatty, T. G., et al. 2015, *ArXiv e-prints*
 Borucki, W. J., Koch, D., Basri, G., et al. 2010, *Science*, 327, 977
 Brown, D. J. A., Anderson, D. R., Armstrong, D. J., et al. 2014, *ArXiv e-prints*
 Burke, C. J., Bryson, S. T., Mullally, F., et al. 2014, *ApJS*, 210, 19
 Collins, K. A., Eastman, J. D., Beatty, T. G., et al. 2014, *AJ*, 147, 39
 Colón, K. D., Ford, E. B., & Morehead, R. C. 2012, *MNRAS*, 426, 342
 Crossfield, I. J. M., Barman, T., Hansen, B. M. S., Tanaka, I., & Kodama, T. 2012, *ApJ*, 760, 140
 Crossfield, I. J. M., Petigura, E., Schlieder, J. E., et al. 2015, *ApJ*, 804, 10
 Daemgen, S., Hormuth, F., Brandner, W., et al. 2009, *A&A*, 498, 567
 Deleuil, M., Deeg, H. J., Alonso, R., et al. 2008, *A&A*, 491, 889
 Désert, J.-M., Charbonneau, D., Torres, G., et al. 2015, *ApJ*, 804, 59
 Dressing, C. D., Adams, E. R., Dupree, A. K., Kulesa, C., & McCarthy, D. 2014, *AJ*, 148, 78
 Everett, M. E., Barclay, T., Ciardi, D. R., et al. 2015, *AJ*, 149, 55
 Fabrycky, D. & Tremaine, S. 2007, *ApJ*, 669, 1298

Table 2: TEP hosts with no detection, radial contrast limits, references to other high-resolution imaging papers if available

Name	5σ detection limit ($\Delta z'$ [mag])				ref.
	0.25''	0.5''	1.0''	2.0''	
55 Cnc	2.90	2.70	3.04	3.85	Roell et al. (2012)
CoRoT-01	3.23	3.81	4.34	4.70	Adams et al. (2013)
CoRoT-07	3.81	4.47	5.26	5.80	Guenther et al. (2013)
CoRoT-24	2.78	3.26	3.44	3.51	Guenther et al. (2013)
EPIC-201367065	4.16	4.98	5.99	6.69	Crossfield et al. (2015)
EPIC-201505350	3.77	4.56	5.43	5.77	
GJ3470	4.01	4.97	5.61	5.96	
HAT-P-09	3.31	4.24	4.77	5.24	
HAT-P-25	3.80	4.72	5.57	5.80	Adams et al. (2013)
HAT-P-33	3.86	4.60	5.29	5.80	Adams et al. (2013); Ngo et al. (2015)
HAT-P-38	3.59	4.46	5.22	5.61	
HAT-P-39	3.28	4.23	4.87	5.32	
HAT-P-42	1.79	2.25	2.95	3.44	
HAT-P-43	3.33	4.18	4.82	5.12	
HAT-P-44	3.73	4.64	5.40	5.67	
HAT-P-45	3.43	4.12	4.75	5.11	
HAT-P-46	3.97	4.64	5.50	5.94	
HAT-P-49	2.83	3.38	3.98	4.64	
KELT-1	3.65	4.19	5.14	5.88	Siverd et al. (2012)
KELT-6	4.07	5.14	6.37	7.19	Collins et al. (2014)
KELT-7	3.80	5.45	6.78	7.70	Bieryla et al. (2015)
Kepler-63	3.59	4.36	5.36	5.73	Sanchis-Ojeda et al. (2013)
KOI-1474	2.79	3.33	3.79	4.16	
Qatar-2	3.59	4.32	5.12	5.47	
TrES-5	2.94	3.48	3.93	4.30	
WASP-30	3.28	3.72	4.63	5.11	
WASP-32	3.47	4.10	5.11	5.56	
WASP-35	3.72	4.42	5.37	5.98	
WASP-43	3.80	4.63	5.37	5.96	
WASP-44	2.85	3.37	4.08	4.47	
WASP-50	3.42	3.97	4.79	5.25	
WASP-54	4.04	5.02	6.22	6.93	
WASP-57	3.56	4.63	5.29	5.46	
WASP-65	3.89	4.73	5.63	6.09	
WASP-69	3.62	4.39	5.13	5.65	
WASP-71	3.59	4.17	5.22	5.94	
WASP-82	3.89	4.80	5.81	6.64	
WASP-84	3.90	4.91	5.81	6.66	
WASP-90	2.83	3.33	3.85	4.36	
WASP-104	3.99	4.88	5.75	6.31	
WASP-106	3.77	4.56	5.41	5.96	

- Faedi, F., Staley, T., Gómez Maqueo Chew, Y., et al. 2013, MNRAS, 433, 2097
 Fischer, D. A., Schwamb, M. E., Schawinski, K., et al. 2012, MNRAS, 419, 2900
 Gandolfi, D., Hébrard, G., Alonso, R., et al. 2010, A&A, 524, A55
 Guenther, E. W., Fridlund, M., Alonso, R., et al. 2013, A&A, 556, A75
 Hartman, J. D., Bakos, G. Á., Béky, B., et al. 2012, AJ, 144, 139
 Horch, E. P., Howell, S. B., Everett, M. E., & Ciardi, D. R. 2014, ApJ, 795, 60
 Hormuth, F., Brandner, W., Hippler, S., & Henning, T. 2008, Journal of Physics Conference Series, 131, 012051
 Howell, S. B., Everett, M. E., Sherry, W., Horch, E., & Ciardi, D. R. 2011, AJ, 142, 19
 Johnson, J. A., Apps, K., Gazak, J. Z., et al. 2011, ApJ, 730, 79
 Kane, S. R., Howell, S. B., Horch, E. P., et al. 2014, ApJ, 785, 93
 Law, N. M., Morton, T., Baranec, C., et al. 2014, ApJ, 791, 35
 Lillo-Box, J., Barrado, D., & Bouy, H. 2012, A&A, 546, A10
 Lillo-Box, J., Barrado, D., & Bouy, H. 2014, A&A, 566, A103
 Maxted, P. F. L., Anderson, D. R., Collier Cameron, A., et al. 2013, PASP, 125, 48
 Mayer, L., Wadsley, J., Quinn, T., & Stadel, J. 2005, MNRAS, 363, 641
 Montet, B. T., Johnson, J. A., Muirhead, P. S., et al. 2015, ApJ, 800, 134
 Moya, A., Bouy, H., Marchis, F., Vicente, B., & Barrado, D. 2011, A&A, 535, A110
 Naoz, S., Farr, W. M., Lithwick, Y., Rasio, F. A., & Teysandier, J. 2011, Nature, 473, 187
 Narita, N., Takahashi, Y. H., Kuzuhara, M., et al. 2012, PASJ, 64, L7
 Ngo, H., Knutson, H. A., Hinkley, S., et al. 2015, ApJ, 800, 138
 Pepper, J., Siverd, R. J., Beatty, T. G., et al. 2013, ApJ, 773, 64
 Pollacco, D. L., Skillen, I., Collier Cameron, A., et al. 2006, PASP, 118, 1407
 Roell, T., Neuhäuser, R., Seifahrt, A., & Mugrauer, M. 2012, A&A, 542, A92
 Sanchis-Ojeda, R., Winn, J. N., Marcy, G. W., et al. 2013, ApJ, 775, 54
 Santerne, A., Moutou, C., Barros, S. C. C., et al. 2012, A&A, 544, L12
 Siverd, R. J., Beatty, T. G., Pepper, J., et al. 2012, ApJ, 761, 123
 Smith, A. M. S., Anderson, D. R., Collier Cameron, A., et al. 2012, AJ, 143, 81
 Wang, J., Fischer, D. A., Xie, J.-W., & Ciardi, D. R. 2014, ApJ, 791, 111
 Winn, J. N., Noyes, R. W., Holman, M. J., et al. 2005, ApJ, 631, 1215
 Wöllert, M., Brandner, W., Bergfors, C., & Henning, T. 2015, A&A, 575, A23
 Wöllert, M., Brandner, W., Reffert, S., et al. 2014, A&A, 564, A10
 Wu, Y. & Murray, N. 2003, ApJ, 589, 605

Table 3: TEP hosts with candidate companions, observing date, inferred astrometric position and flux ratio in the observed pass-bands. In the last column we indicate whether the companion was announced previously.

Name	Date of obs.	Sep ["]	PA [°]	$\Delta i'$ [mag]	$\Delta z'$ [mag]	new?
CoRoT-02	21.10.2014	4.109 ± 0.025	208.56 ± 0.14	3.35 ± 0.15	3.07 ± 0.15	
CoRoT-03	21.10.2014	5.221 ± 0.013	175.62 ± 0.55	3.39 ± 0.25	3.48 ± 0.36	
CoRoT-11	21.10.2014	2.540 ± 0.005	307.38 ± 0.17	2.27 ± 0.09	2.14 ± 0.09	
HAT-P-15 south west	21.10.2014	6.253 ± 0.026	233.42 ± 1.54	7.17 ± 0.49	6.74 ± 0.45	yes
	07.03.2015	6.136 ± 0.014	235.71 ± 1.02	–	6.79 ± 0.22	
HAT-P-15 south	07.03.2015	7.091 ± 0.014	194.23 ± 1.02	–	6.66 ± 0.20	yes
HAT-P-20	21.10.2014	6.925 ± 0.012	321.10 ± 0.11	2.01 ± 0.08	1.67 ± 0.08	
HAT-P-24	06.03.2015	4.965 ± 0.008	171.32 ± 0.60	6.01 ± 0.18	5.80 ± 0.24	
HAT-P-27/WASP-40	27.06.2013 †	0.656 ± 0.021	25.74 ± 1.19	*	*	yes
	09.03.2015	0.644 ± 0.007	28.40 ± 1.86	–	4.44 ± 0.32	
HAT-P-28	21.10.2014	0.972 ± 0.019	212.34 ± 2.05	6.2 :	4.09 ± 0.27	yes
HAT-P-29	06.03.2015	3.276 ± 0.104	160.71 ± 1.36	7.93 ± 0.25	6.73 ± 0.35	yes
	21.10.2014	3.285 ± 0.050	161.64 ± 2.36	6.31 ± 0.42	6.11 ± 0.58	
HAT-P-30	09.03.2015	3.842 ± 0.007	4.25 ± 0.14	4.50 ± 0.06	4.03 ± 0.06	
HAT-P-32	09.03.2015	2.930 ± 0.009	110.84 ± 0.43	–	5.43 ± 0.16	
HAT-P-35	09.03.2015	0.933 ± 0.010	139.75 ± 1.23	5.09 ± 0.24	* ^o	yes
HAT-P-41	21.10.2014	3.640 ± 0.011	184.00 ± 0.15	3.72 ± 0.13	3.61 ± 0.17	
HAT-P-54	21.10.2014	4.531 ± 0.062	135.95 ± 1.96	5.68 ± 0.53	5.69 ± 0.59	yes
	06.03.2015	4.593 ± 0.010	135.82 ± 0.27	*	5.61 ± 0.26	
KELT-2	21.10.2014	2.402 ± 0.008	332.85 ± 0.15	3.19 ± 0.09	3.13 ± 0.09	
	06.03.2015	2.396 ± 0.007	332.81 ± 0.14	2.82 ± 0.15	3.02 ± 0.15	
KELT-3	06.03.2015	3.762 ± 0.009	42.05 ± 0.23	3.93 ± 0.15	3.60 ± 0.15	
Kepler-13	21.10.2014	1.159 ± 0.003	280.02 ± 0.22	0.24 ± 0.02	0.26 ± 0.03	
Kepler-89	21.10.2014	7.316 ± 0.028	108.59 ± 0.11	3.66 ± 0.18	3.37 ± 0.23	yes
KIC10905746	21.10.2014	4.053 ± 0.007	98.61 ± 0.12	2.18 ± 0.16	1.91 ± 0.16	
LHS-6343	21.10.2014	0.723 ± 0.006	119.86 ± 1.30	2.29 ± 0.24	1.66 ± 0.13	
TrES-4	07.03.2015	1.583 ± 0.019	0.69 ± 0.31	4.06 ± 0.07	4.04 ± 0.09	
WASP-11	21.10.2014	0.374 ± 0.013	219.75 ± 0.79	2.94 ± 0.50	2.93 ± 0.45	
	06.03.2015	0.383 ± 0.033	218.33 ± 1.41	3.18 ± 0.26	2.91 ± 0.20	
WASP-12	06.03.2015	1.078 ± 0.008	250.08 ± 0.55	4.13 ± 0.10	3.68 ± 0.08	
WASP-14	06.03.2015	1.425 ± 0.024	102.39 ± 0.40	7.14 ± 0.22	5.95 ± 0.10	
WASP-33	21.10.2014	1.920 ± 0.012	275.87 ± 0.71	9.7 :	7.23 ± 0.22	
WASP-36	09.03.2015	4.845 ± 0.017	67.23 ± 0.95	8.5 :	6.45 ± 0.59	
WASP-56	06.03.2015	3.424 ± 0.009	113.35 ± 0.18	6.85 ± 0.24	5.95 ± 0.22	yes
WASP-70	21.10.2014	3.195 ± 0.029	167.83 ± 0.19	2.62 ± 0.18	2.49 ± 0.20	
WASP-76	21.10.2014	0.425 ± 0.012	216.90 ± 2.93	2.51 ± 0.25	2.85 ± 0.33	yes
WASP-77	21.10.2014	3.282 ± 0.007	154.02 ± 0.12	1.80 ± 0.06	1.63 ± 0.06	
WASP-85	09.03.2015	1.470 ± 0.003	100.09 ± 0.19	0.89 ± 0.01	0.85 ± 0.01	
WASP-103	07.03.2015	0.242 ± 0.016	132.66 ± 2.74	3.11 ± 0.46	2.59 ± 0.35	yes
XO-3	06.03.2015	6.078 ± 0.081	297.21 ± 0.13	8.13 ± 0.28	7.93 ± 0.25	

–: no observation in this band

*: companion candidate was too weak for flux measurement

†: The source was first not identified by us (Wöllert et al. 2015), but after the new observation with better contrast it could be located.

^o: The exposure time in z' was five times smaller than the one in i' .

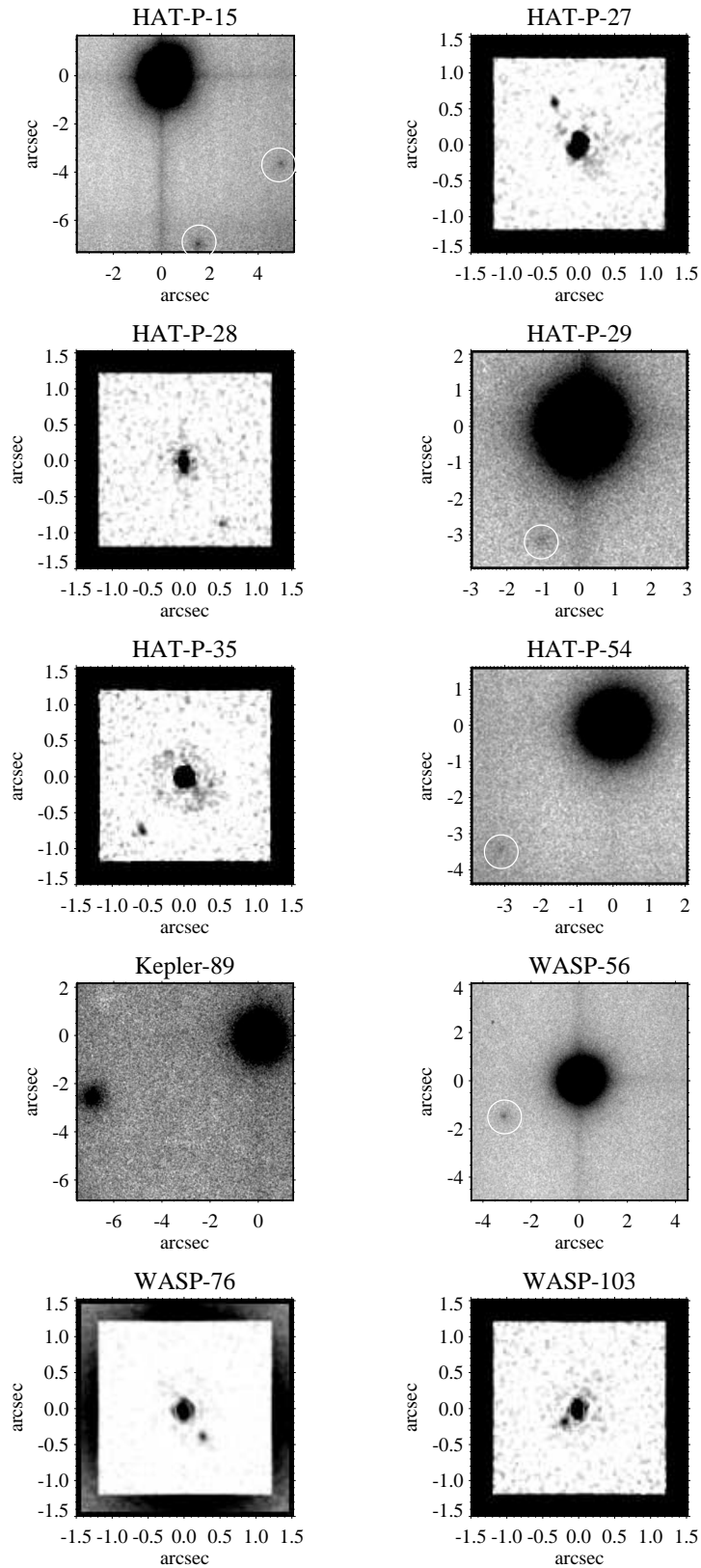


Fig. 1: The z' filter images of the 10 exoplanet host stars for which new companion candidates have been detected with exception of HAT-P-35 for which the i' -image is shown. The grey scale is proportional to the square root of the count. To improve the visibility of the close companions to HAT-P-27, HAT-P-28, HAT-P-35, WASP-76, and WASP-103, we additionally applied unsharp masking. The orientation is identical for all images with North up and East to the left.